

Fig. 4.5: EIS test linearity vs. final model nonlinearity

the beginning to the end of the test, invalidating the results obtained. The maximum frequency limit is defined by the maximum operating frequency at which the fuel cell will be operated, i.e. the rise time of the most abrupt transitory, which will not exceed the kHz frequencies. With these considerations in mind, the frequency interval selected is 0.5 Hz-6 kHz as with these frequencies the tests render the results needed. In order to obtain solid data, 20 cycles are applied for each frequency and 40 points per decade registered.

4.2.3. Experimental setup

To carry out the EIS tests the following equipment has been used:

- Impedance analyzer (Solartron 1260).
- DC electronic load (Chroma 63201: 80 V, 300 A).
- DC power source (Sorensen SGI: 60 V, 167 A).
- LEM LA 55-P current transducer.
- ± 15 V power source for transducer supply.
- Computer.
- Nexa Ballard fuel cell.

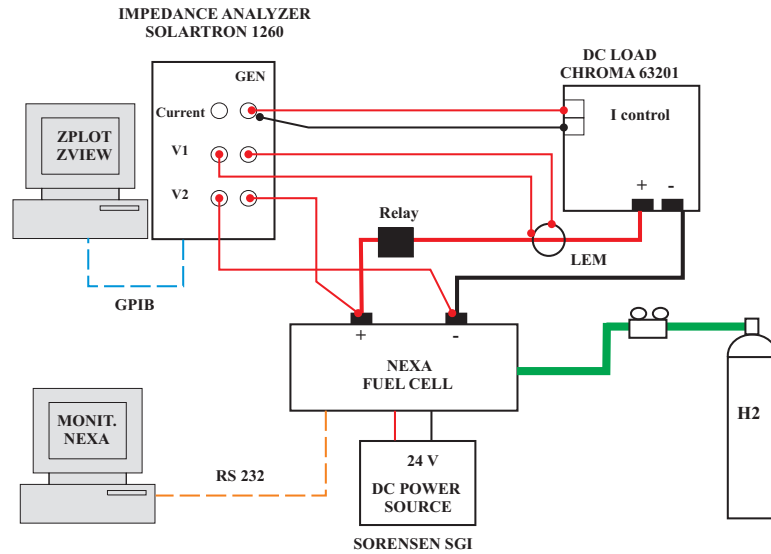


Fig. 4.6: Experimental setup for Nexa fuel cell EIS tests

The wiring diagram and a photograph of the EIS tests experimental setup are presented in Figs. 4.6 and 4.7. The tests are controlled by the impedance analyzer Solartron 1260, which through the software ZPlot sends an analogical signal to the electronic load representing the dc+ac current forced at the output of the fuel cell. The current and voltage are measured through the terminals V1 and V2 and sent to the impedance analyzer, which can then calculate the complex impedance by extracting the ac components of the current and voltage. The impedance measurements takes into account the power cables included in the Nexa fuel cell for its connection.

4.3. EIS tests results: fuel cell impedance model

The data obtained during the EIS tests is then processed with the software ZView, which represents the Nyquist and Bode plots for the complex impedance calculated, as presented in Fig. 4.8. The abscissa axis Z' represents the real part of the fuel cell complex impedance, whilst the ordinate axes Z'' represents the imaginary part. The frequency sweep starts at the minimum frequency, which corresponds to the farthest point in the right hand side of the Nyquist plot and increases as the test develops towards the left hand side points. Negative values of Z'' correspond to the capacitance behavior

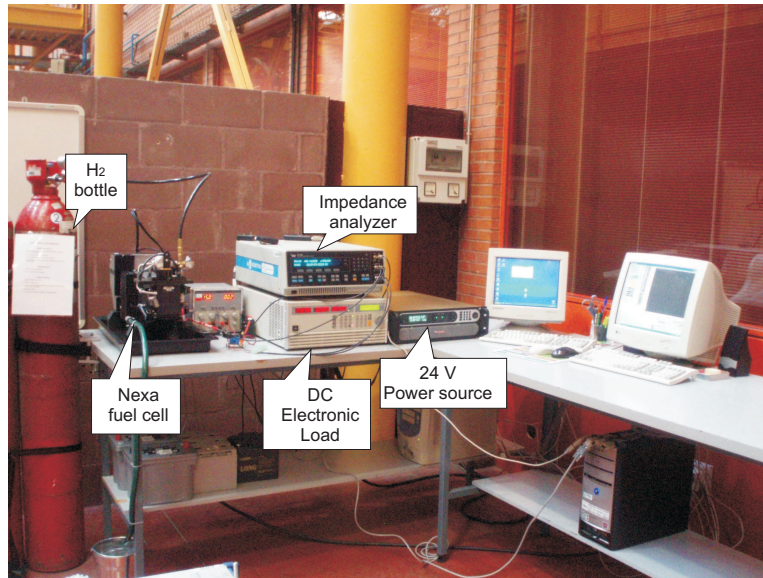


Fig. 4.7: Experimental setup photograph

of the fuel cell, whilst positive values correspond to inductive behavior. The resonance frequency point is defined as the frequency in which the capacitive and inductive impedances cancel each other, and therefore the fuel cell impedance becomes purely resistive ($Z''=0$). As it can be observed in Fig. 4.8, the complex impedance of the fuel cell decreases for increasing currents up to 40 A and increases for higher currents. This phenomenon is also described in [54], and is present at high currents, when the mass transfer is dominant.

To obtain an electric model, the impedance values obtained through the EIS tests must be fitted to a particular electric circuit. The software ZView allows to test between any electric circuit defined by the user with the elements included in its library. Therefore, a wide combination of circuits can be tested. Fig. 4.9 presents the information returned by ZView for the 10 A test, which includes the parameters, its absolute values and error between the experimental and simulated equivalent circuit. The circuit presented is formed by a series inductance which represents the inductive behavior of the system at high frequencies, a series resistance which reflects the ionic resistance of the membrane. The circuit also presents an R_1CPE network. The constant phase element CPE, as explained by [46], [82] and [54], is a fictitious element which can model diffusion phenomena, roughness of electrodes or inhomogeneous distribution of reactants on the surface. The CPE can also try

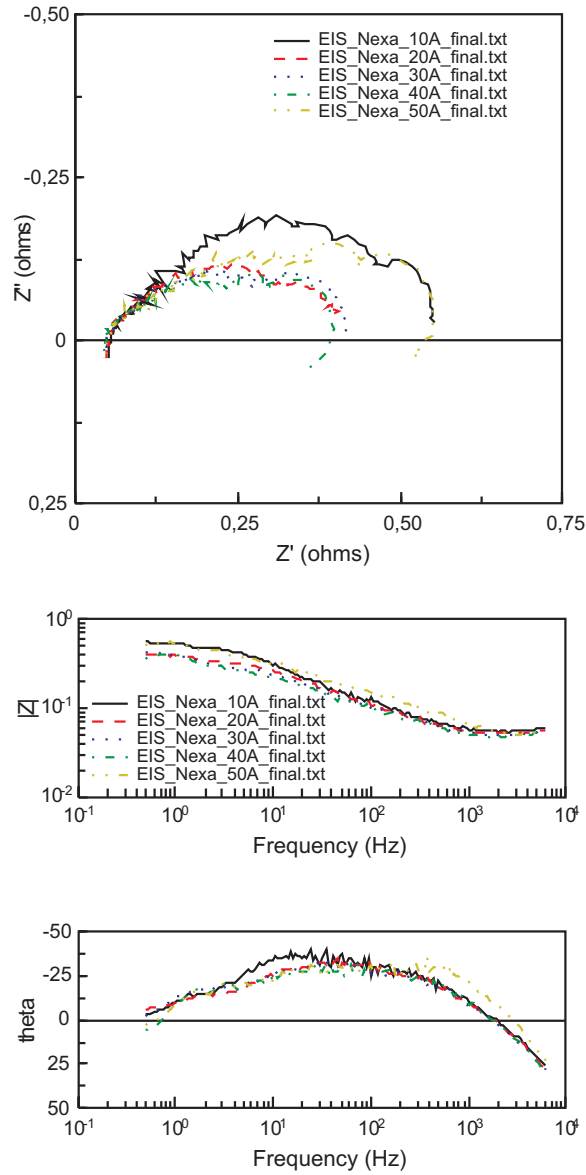
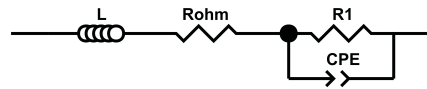


Fig. 4.8: Nexa fuel cell Nyquist and Bode plots



Element	Freedom	Value	Error	Error %
L	Free(+)	8,1432E-7	2,0041E-8	2,4611
Rohm	Free(+)	0,049393	0,00043111	0,87282
R1	Free(+)	0,56896	0,0065807	1,1566
CPE-T	Free(+)	0,15304	0,0042221	2,7588
CPE-P	Free(+)	0,67358	0,0049499	0,73486

Fig. 4.9: Fuel cell parameters rendered by ZView

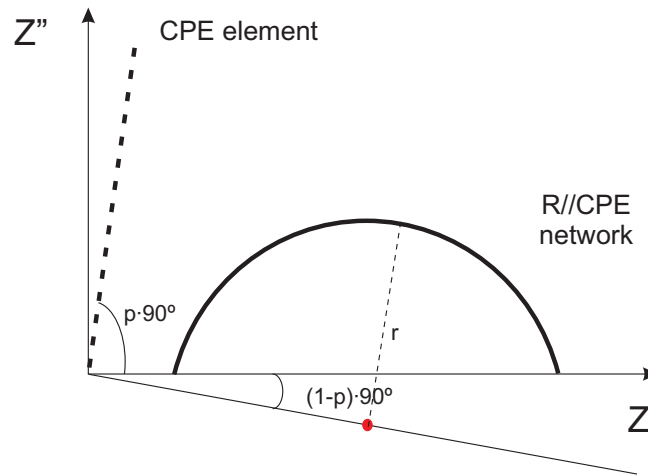


Fig. 4.10: CPE and R-CPE Nyquist plots

to represent the fractal dimension of surfaces which are not 2D or 3D, but an intermediate value. In this Thesis, we have used a CPE due to the fact that it takes into account all these phenomena and combined with a resistance can reproduce the semicircle that appears in the Nyquist plot, whose center does not lay on the abscissa axis, but in a lower position, as depicted in Fig. 4.10. Mathematically, the CPE impedance can be described as:

$$\frac{1}{Z} = Y = T_{cpe} \cdot (j \cdot \omega)^p \quad (4.1)$$

The parameter p varies between 0.5 and 1, therefore the CPE Nyquist plot is not a vertical line as a capacitor, but inclined with a $p \cdot 90^\circ$ angle. If p is 1, the equation is identical to a capacitor equation. However, a CPE is not a physical element, and cannot be described by a single electric equation, hence, an equivalent capacitor C_1 can be calculated with (4.1) for the R-CPE network, where T_{cpe} and p are the CPE parameters.

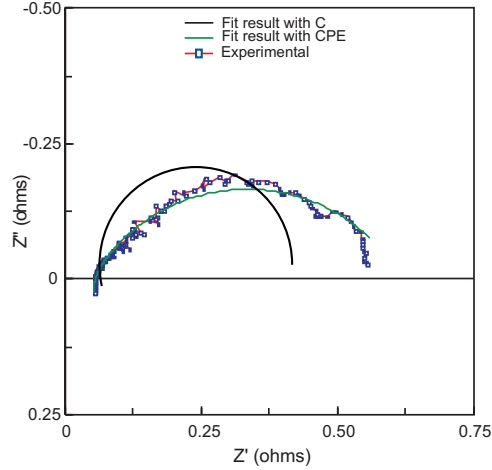


Fig. 4.11: Difference in the C or CPE fitting

$$C_1(F) = T_{cpe} \cdot (\omega_{\max})^{p-1} = \frac{(T_{cpe} \cdot R)^{1/p}}{R} \quad (4.2)$$

The value of this equivalent capacitor is different from the one obtained if the Nyquist plot is directly fitted to an RC network instead of an R-CPE network. For instance, for the test at 10 A, the value of C was a 40 % smaller than the equivalent capacitor calculated after fitting the CPE. The different fit for each option is shown in Fig. 4.11. This advantage of the CPE over the capacitor is also commented, but not proved, by [59].

4.3.1. Fuel cell equivalent circuit

Therefore, the equivalent circuit obtained is shown in Fig. 4.12, where E is the fuel cell internal voltage, R_{ohm} the contact resistance and R_1C_1 the network which emulates the double layer capacitor. The voltage on terminals of the fuel cell is U_{fc} .

A study of the dependency of each parameter of the equivalent circuit as polynomial equations with the current is carried out. To prove this dependency a statistical analysis is carried out with the statistical software Statgraphics. Statgraphics is a statistical program developed by Statpoint Technologies Inc. which is a 32 bit program which runs under Windows.

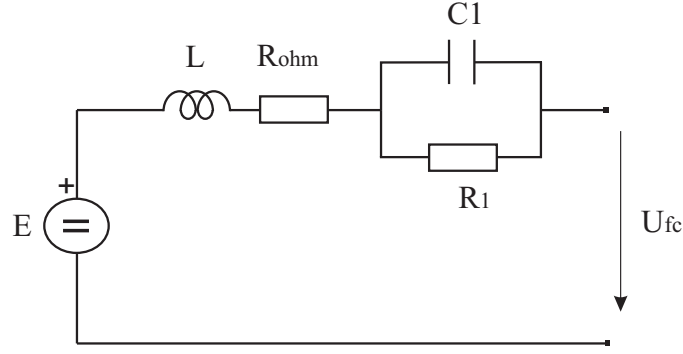


Fig. 4.12: Fuel cell equivalent circuit

An example of the information returned by Statgraphics for R_1 is presented in Fig. 4.13. The information yielded by Statgraphics includes the observed vs. predicted plot, in which the model points should be as near as possible to the line with slope 1 shown. It can be observed that the predicted vs. observed values adjust very satisfactorily to the 45° line.

The electrical equations which can be obtained from Fig. 4.12 are presented in (4.3) and (4.4):

$$\begin{aligned}
 L (H) &= 1,33 \cdot 10^{-6} - 5,23 \cdot 10^{-8} \cdot I + 6,41 \cdot 10^{-10} \cdot I^2 + 5,09 \cdot 10^{-12} \cdot I^3 \\
 R_{ohm} (\Omega) &= 0,05 - 7,83 \cdot 10^{-6} \cdot I + 1,97 \cdot 10^{-5} \cdot I^2 - 2,39 \cdot 10^{-7} \cdot I^3 \\
 R_1 (\Omega) &= 0,76 - 0,02 \cdot I + 1,80 \cdot 10^{-4} \cdot I^2 + 3,97 \cdot 10^{-6} \cdot I^3 \\
 C_1 (F) &= 0,12 - 0,01 \cdot I + 7,27 \cdot 10^{-4} \cdot I^2 - 1,45 \cdot 10^{-6} \cdot I^3 + 9,36 \cdot 10^{-8} \cdot I^4
 \end{aligned} \tag{4.3}$$

$$\begin{aligned}
 U_{fc} (V) &= E - R_{ohm} \cdot I - \left(I - C_1 \cdot \frac{dU_{C1}}{dt} \right) \cdot R_1 \\
 E (V) &= N \cdot \left[E_0 + \frac{RT}{2F} \cdot \left(\ln \frac{p_{H_2} \cdot \sqrt{p_{O_2}}}{p_{H_2O}} \right) \right]
 \end{aligned} \tag{4.4}$$

N is the number of cells in series (47), E_0 is the standard no load fuel cell voltage, R the universal gas constant, T the stack temperature, F the Faraday constant, p_{H_2} the partial pressure of hydrogen at the anode, p_{O_2} the partial pressure of oxygen at the cathode and p_{H_2O} the partial pressure of water formed at the cathode. The stack temperature is highly dependant on the current generated by the fuel cell, and will be demonstrated later.

```

Multiple Regression Analysis
-----
Dependent variable: R1
-----
Parameter          Estimate          Standard Error          T Statistic          P-Value
-----
CONSTANT           -0,881369         0,0776897              -11,3447             0,0560
I                   0,132302          0,0101552              13,028              0,0488
I^2                -0,00438669       0,000376927            -11,638             0,0546
I^3                0,0000451043      0,00000416174          10,8378             0,0586
-----

Analysis of Variance
-----
Source              Sum of Squares      Df  Mean Square      F-Ratio      P-Value
-----
Model               0,0829511          3   0,0276504        110,86       0,0687
Residual            0,000249409        1   0,000249409
-----
Total (Corr.)       0,0832006          4
-----

R-squared = 99,7002 percent
R-squared (adjusted for d.f.) = 98,8009 percent
Standard Error of Est. = 0,0157927
Mean absolute error = 0,00604027
Durbin-Watson statistic = 3,57143
    
```

The StatAdvisor

The output shows the results of fitting a multiple linear regression model to describe the relationship between R1 and 3 independent variables. The equation of the fitted model is

$$R1 = -0,881369 + 0,132302 \cdot I - 0,00438669 \cdot I^2 + 0,0000451043 \cdot I^3$$

Since the P-value in the ANOVA table is less than 0.10, there is a statistically significant relationship between the variables at the 90% confidence level.

The R-Squared statistic indicates that the model as fitted explains 99,7002% of the variability in R1. The adjusted R-squared statistic, which is more suitable for comparing models with different numbers of independent variables, is 98,8009%. The standard error of the estimate shows the standard deviation of the residuals to be 0,0157927. This value can be used to construct prediction limits for new observations by selecting the Reports option from the text menu. The mean absolute error (MAE) of 0,00604027 is the average value of the residuals. The Durbin-Watson (DW) statistic tests the residuals to determine if there is any significant correlation based on the order in which they occur in your data file. Since the DW value is greater than 1.4, there is probably not any serious autocorrelation in the residuals.

In determining whether the model can be simplified, notice that the highest P-value on the independent variables is 0,0586, belonging to I^3 . Since the P-value is less than 0.10, that term is statistically significant at the 90% confidence level. Depending on the confidence level at which you wish to work, you may or may not decide to remove I^3 fr

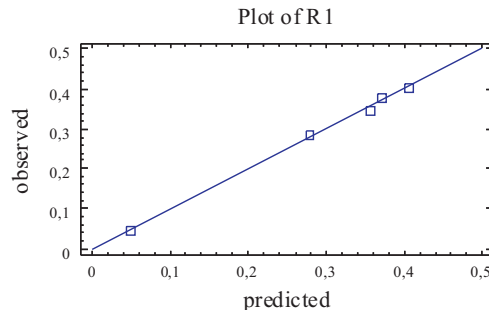


Fig. 4.13: Information returned by Statgraphics for $R1$

The partial pressures can be obtained through the ideal gas law, which is, for example, applied to hydrogen as:

$$p_{H_2} \cdot V_{an} = n_{H_2} \cdot R \cdot T \quad (4.5)$$

V_{an} [83] is the volume of gas present in the anode and n_{H_2} the moles of hydrogen. If (4.5) is derived respect to time (4.6) is obtained.

$$\frac{dp_{H_2}}{dt} = \frac{RT}{V_{an}} \cdot q_{H_2} = \frac{RT}{V_{an}} \cdot (q_{H_2}^{in} - q_{H_2}^{out} - q_{H_2}^r) \quad (4.6)$$

q_{H_2} is the flow of hydrogen in (moles/s).

$q_{H_2}^{in}$ is the flow of hydrogen moles which enter the stack.

$q_{H_2}^{out}$ is the flow of hydrogen moles which leave the stack.

$q_{H_2}^r$ is the flow of hydrogen moles which react in the stack.

The flow of hydrogen and air moles which enter the stack can be measured with a flow meter. If no flow meter is used, as in this Thesis, the flow of moles can be calculated indirectly with (9) known the flow of moles which have reacted and the stoichiometric relationship SR of the gas. The gas SR reflects the gas excess which should be supplied to the reaction in order to obtain a satisfactory reaction. Here we have used the SR approximation suggested by [83].

$$\begin{aligned} SR &= \frac{q_{H_2}^{in}}{q_{H_2}^r} \\ SR_{H_2} &= 1,02875 + 0,00412546 \cdot I \\ SR_{O_2} &= 5,51131 - 0,138273 \cdot I + 0,00146051 \cdot I^2 \\ q_{H_2}^r &= \frac{I}{2 \cdot F} \end{aligned} \quad (4.7)$$

Equation (4.8) is obtained if (4.7) is substituted in (4.6).

$$\begin{aligned} \frac{dp_{H_2}}{dt} &= \frac{RT}{V_{an}} \cdot q_{H_2} = \frac{RT}{V_{an}} \cdot (SR_{H_2} \cdot q_{H_2}^r - q_{H_2}^r) = \\ &= \frac{RT}{V_{an}} \cdot (SR_{H_2} - 1) \cdot \frac{I}{2F} \end{aligned} \quad (4.8)$$

Similar equations can be deduced for the oxygen and water partial pressures. Known these partial pressures and substituted in (4.4) allows calculating the fuel cell output voltage.

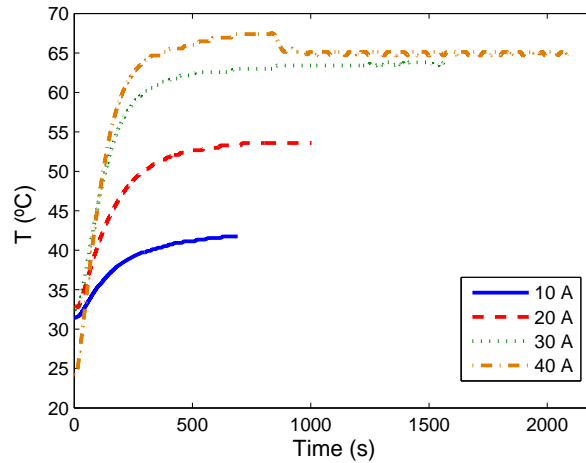


Fig. 4.14: Temperature evolution for different current steps

4.3.2. Temperature model

As pointed out before, the fuel cell output voltage is influenced by the stack temperature [8] whilst the temperature depends on the current supplied by the fuel cell [52], [53]. The temperature is controlled by the fuel cell control system, and includes a fan for cooling purposes. To investigate the dependency of temperature with current, current steps for 10, 20 and 30 A were applied to the fuel cell until the stationary temperature was reached. The temperature evolution for these current steps is presented in Fig. 4.14.

With these results, the final temperature for each current and thermal time constant can be calculated. This thermal time constant is influenced by the cooling fan, which is normally at a certain percentage duty cycle in order to, not only to cool the stack, but also dilute hydrogen that is purged from the fuel cell during normal operation [28]. The thermal time constant is obtained as the time elapsed until the 63% of the steady-state value is reached. Again, the software Statgraphics is used to obtain the relationship between current and the thermal time constant. Fig. 4.15 presents the results and observed vs. predicted curve, which shows a good agreement:

$$\tau (s) = 181,624 + 0,8028 \cdot I - 0,0532 \cdot I^2 \quad (4.9)$$

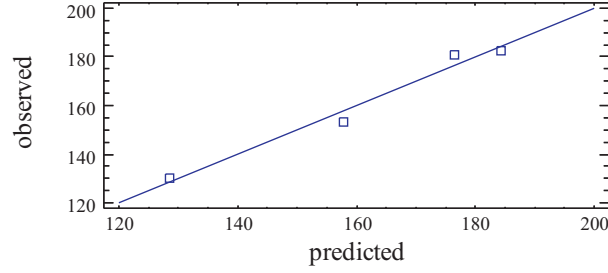


Fig. 4.15: Statgraphics result for the thermal time constant

Whilst the dependency of the final temperature with the current can be expressed as:

$$T_f (\text{°C}) = 24,4975 + 1,9058 \cdot I - 0,0531 \cdot I^2 \quad (4.10)$$

Known the stationary temperature and the time constant, the temperature evolution with time and current for an initial temperature T_0 (room temperature) can be obtained with:

$$T (\text{°C}) = T_0 + (T_f - T_0) \cdot (1 - e^{-t/\tau}) \quad (4.11)$$

In order to validate the temperature model proposed, the current profile of Fig. 4.16 is applied to the fuel cell, whilst the temperature and fan duty cycle are measured. The results can be observed in Fig. 4.17.

It can be observed in Fig. 4.17 that the simulated temperature follows the measured values, except for high currents, which provokes the model to deviate. This difference is due to the fact that the fan increases its duty cycle nearly a 20 % when the stack temperature rises above 65°C, thus changing the heat transfer rate of the stack. On the contrary, the modeled temperature keeps rising with a slightly different time constant. This difference affects the subsequent points. When the duty cycle returns to near a 35 %, the simulated and experimental temperatures match again.

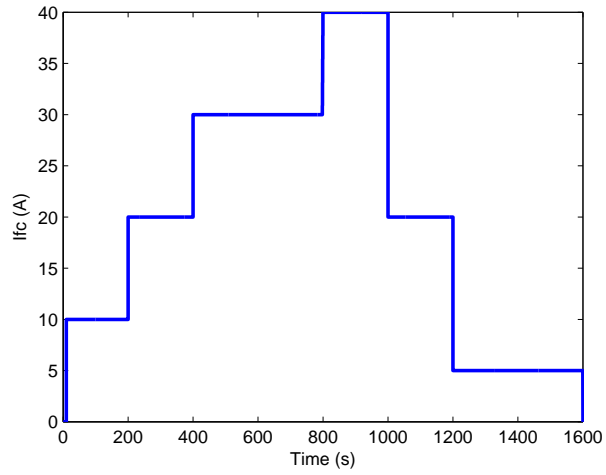


Fig. 4.16: Current profile applied to fuel cell and model

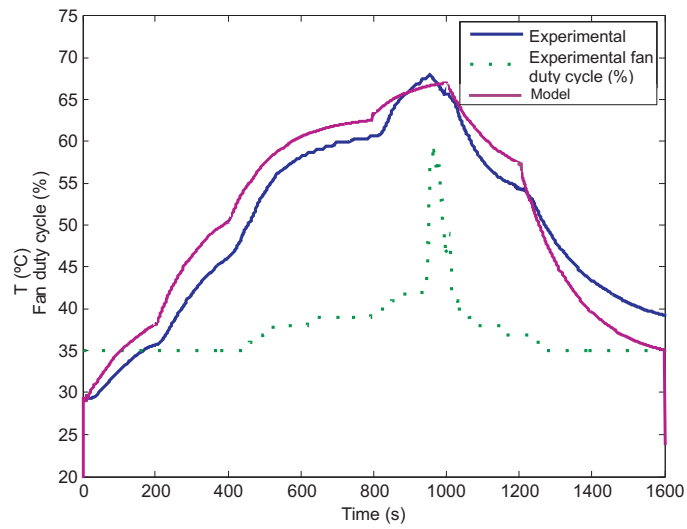


Fig. 4.17: Temperature model validation

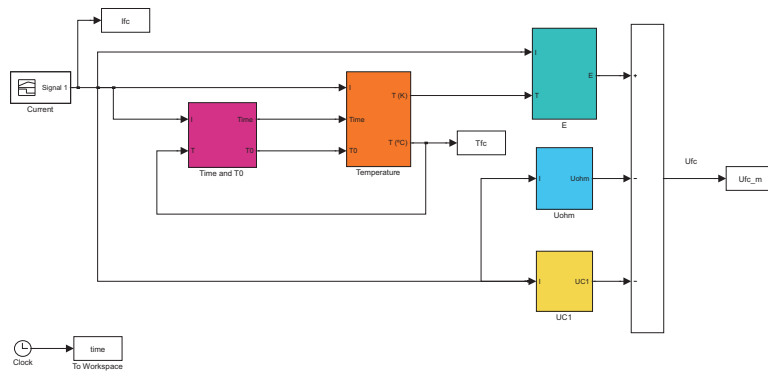


Fig. 4.18: Fuel cell Matlab/Simulink model

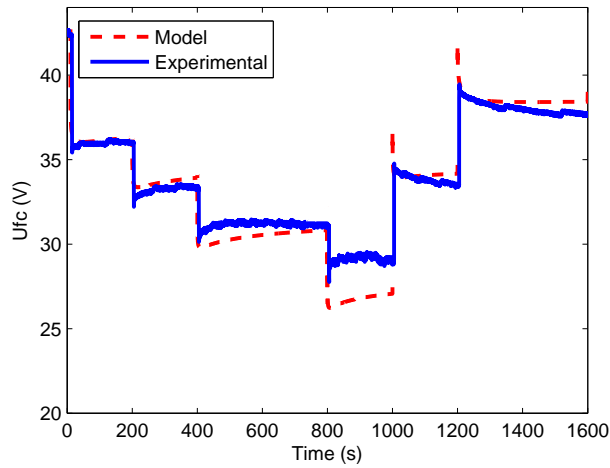


Fig. 4.19: Complete model validation

4.3.3. Complete model validation

The electrical equivalent circuit equations and temperature model were programmed in Matlab/Simulink, as shown in Fig. 4.18. The same current profile in Fig. 4.16 was applied to the fuel cell and the voltage was monitored. The comparison between experimental and modeled values are presented in Fig. 4.19.

In general the model yields a good approximation of the experimental values. Here also, a maximum difference of an 8% appears during the maximum current pulse, which provokes the increase of the stack temperature and fan duty cycle. The temperature affects the fuel cell impedance [53], [52], especially at very high temperatures, as in this case.

4.4. Per-unit approach

A per unit system pursues the representation of electric variables as dimensionless values referred to a set of base values. The electric variables in a power system are power, voltage, current and impedance and a mathematical relationship between them can be found. As there are four different, but interdependent variables, it is a two degree of freedom system in which once two of base values are defined, the other two can be obtained with (4.12).

$$\begin{aligned} P &= U \cdot I \\ U &= I \cdot Z \end{aligned} \tag{4.12}$$

The definition of the base values is an arbitrary decision; however, for a particular component it is usual to select the its rated values as base values. For example, in a generator with rated 200 MVA and 20 kV voltage, the base power and voltage can coincide with its rated values. Hence, the base current and impedance can be calculated as:

$$\begin{aligned} I_b &= \frac{S_b}{\sqrt{3} \cdot U_b} = \frac{200 \cdot 10^6}{\sqrt{3} \cdot 20 \cdot 10^3} = 5773,5 \text{ A} \\ Z_b &= \frac{U_b^2}{S_b} = \frac{(20 \cdot 10^3)^2}{200 \cdot 10^6} = 2 \text{ } \Omega \end{aligned} \tag{4.13}$$

For this example, if an element consumes 20 MW, the p.u. power will be 0.1 p.u, which gives an understandable measure of the power consumed compared with the rated value.

As it was pointed before, power systems may present different voltage levels; therefore, the base voltage will be different for each area. The power element which separates each different base voltage region is a power transformer, which establishes the voltage levels depending on the number of turns of its windings. Fuel cells are not directly connected to a power transformer, but to an electronic power converter, which carries out the same function of voltage area definition as the power transformer.

4.4.1. Steady-state per-unit system for a fuel cell

In this work we will present a per-unit model for a Ballard Nexa 1.2 kW fuel cell. The voltage and power curve are depicted in Fig. 4.20. As it can be

Base power	Base current	Base voltage	Base impedance
1.2 kW	45 A	26.67 V	0.59267 W

Table 4.1: Steady-state base magnitudes

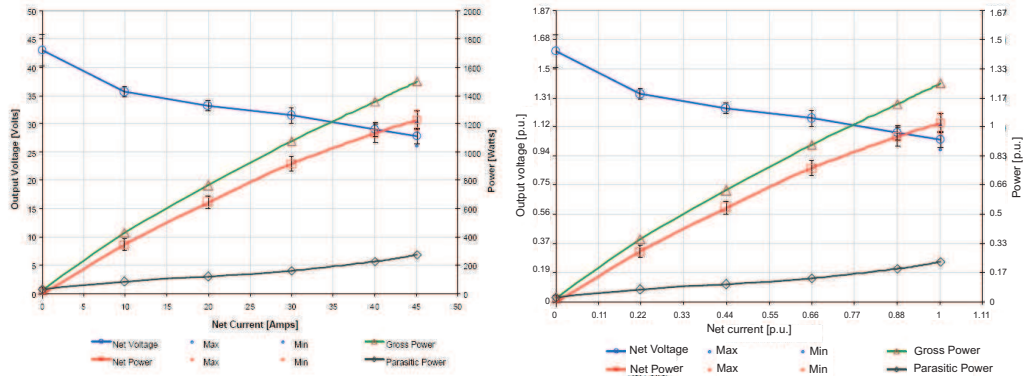


Fig. 4.20: Nexa fuel cell voltage and power characteristic in absolute (left) [28] and p.u. values (right)

observed, the maximum power obtained is 1.2 kW at 45 A of current. The curves have not been depicted for higher currents as the power and voltage values would decrease nonlinearly and provoke a low efficient operation. As the rated power is 1.2 kW, this value will be chosen as the base power. Likewise, the base current can be 45 A. However, this decision is arbitrary and other values may be considered. Known these two base values, the rest of the base values can be calculated according to (4.12). The whole set of base values are presented in Table 4.1. With these base values, the absolute curve in Fig. 4.20 can be regarded from a different perspective if the voltage, current, and power values are expressed in p.u. values, as done in the right side of Fig. 4.20.

With a simple glance to the p.u. curve of Fig. 4.20 it is possible to know, e.g. how far each point is from the rated operation point (1 p.u.). This cannot be done when absolute values are used, as seen in the absolute curve of Fig. 4.20. Therefore, the curves are the same, but the language in which they are expressed highlight information which otherwise would go unnoticed.